Research Article | Vol. 25, No. 6 | 20 Mar 2017 | OPTICS EXPRESS 6832

Optics EXPRESS

# Novel birefringence interrogation for Sagnac loop interferometer sensor with unlimited linear measurement range

HAIJUN HE, LIYANG SHAO,* HENG QIAN, XINPU ZHANG, JIAWEI LIANG, BIN LUO, WEI PAN, AND LIANSHAN YAN

*Center for Information Photonics & Communications, School of Information Science & Technology, Southwest Jiaotong University, Chengdu, Sichuan, 611756, China*
*lyshao@home.swjtu.edu.cn;*

**Abstract:** A novel demodulation method for Sagnac loop interferometer based sensor has been proposed and demonstrated, by unwrapping the phase changes with birefringence interrogation. A temperature sensor based on Sagnac loop interferometer has been used to verify the feasibility of the proposed method. Several tests with 40 °C temperature range have been accomplished with a great linearity of 0.9996 in full range. The proposed scheme is universal for all Sagnac loop interferometer based sensors and it has unlimited linear measurable range which overwhelming the conventional demodulation method with peak/dip tracing. Furthermore, the influence of the wavelength sampling interval and wavelength span on the demodulation error has been discussed in this work. The proposed interrogation method has a great significance for Sagnac loop interferometer sensor and it might greatly enhance the availability of this type of sensors in practical application.



**OCIS codes:** (060.2370) Fiber optics sensors; (060.2420) Fibers, polarization-maintaining; (120.5790) Sagnac effect; (260.1440) Birefringence; (060.2270) Fiber characterization.

## References and links

1. E. De la Rosa, L. A. Zenteno, A. N. Starodumov, and D. Monzon, "All-fiber absolute temperature sensor using an unbalanced high-birefringence Sagnac loop," Opt. Lett. **22**(7), 481–483 (1997).
2. D. H. Kim and J. Kang, "Sagnac loop interferometer based on polarization maintaining photonic crystal fiber with reduced temperature sensitivity," Opt. Express **12**(19), 4490–4495 (2004).
3. D. S. Moon, B. H. Kim, A. Lin, G. Sun, Y.-G. Han, W.-T. Han, and Y. Chung, "The temperature sensitivity of Sagnac loop interferometer based on polarization maintaining side-hole fiber," Opt. Express **15**(13), 7962–7967 (2007).
4. Y. Liu, B. Liu, X. Feng, W. Zhang, G. Zhou, S. Yuan, G. Kai, and X. Dong, "High-birefringence fiber loop mirrors and their applications as sensors," Appl. Opt. **44**(12), 2382–2390 (2005).
5. X. Dong, H. Y. Tam, and P. Shum, "Temperature-insensitive strain sensor with polarization-maintaining photonic crystal fiber based Sagnac interferometer," Appl. Phys. Lett. **90**(15), 151113 (2007).
6. L. Y. Shao, X. Zhang, H. He, Z. Zhang, X. Zou, B. Luo, W. Pan, and L. Yan, "Optical fiber temperature and torsion sensor based on Lyot-Sagnac interferometer," Sensors (Basel) **16**(10), 1774 (2016).
7. H. Y. Fu, H. Y. Tam, L. Y. Shao, X. Dong, P. K. Wai, C. Lu, and S. K. Khijwania, "Pressure sensor realized with polarization-maintaining photonic crystal fiber-based Sagnac interferometer," Appl. Opt. **47**(15), 2835–2839 (2008).
8. P. Zu, C. C. Chan, G. W. Koh, W. S. Lew, Y. Jin, H. F. Liew, W. C. Wong, and X. Dong, "Enhancement of the sensitivity of magneto-optical fiber sensor by magnifying the birefringence of magnetic fluid film with Loyt-Sagnac interferometer," Sens. Actuators B Chem. **191**, 19–23 (2014).
9. O. Frazão, B. V. Marques, P. Jorge, J. M. Baptista, and J. L. Santos, "High birefringence D-type fibre loop mirror used as refractometer," Sens. Actuators B Chem. **135**(1), 108–111 (2008).
10. W. Qian, C. L. Zhao, S. He, X. Dong, S. Zhang, Z. Zhang, S. Jin, J. Guo, and H. Wei, "High-sensitivity temperature sensor based on an alcohol-filled photonic crystal fiber loop mirror," Opt. Lett. **36**(9), 1548–1550 (2011).
11. B. H. Kim, S. H. Lee, A. Lin, C. L. Lee, J. Lee, and W. T. Han, "Large temperature sensitivity of Sagnac loop interferometer based on the birefringent holey fiber filled with metal indium," Opt. Express **17**(3), 1789–1794 (2009).
12. L. Shao, Y. Luo, Z. Zhang, X. Zou, B. Luo, W. Pan, and L. Yan, "Sensitivity-enhanced temperature sensor with cascaded fiber optic Sagnac interferometers based on Vernier-effect," Opt. Commun. **336**, 73–76 (2015).

#285293 https://doi.org/10.1364/OE.25.006832
Journal © 2017 Received 19 Jan 2017; revised 8 Mar 2017; accepted 10 Mar 2017; published 15 Mar 2017

Optics EXPRESS

13. T. Martynkien, G. Statkiewicz-Barabach, J. Olszewski, J. Wojcik, P. Mergo, T. Geernaert, C. Sonnenfeld, A. Anuszkiewicz, M. K. Szczurowski, K. Tarnowski, M. Makara, K. Skorupski, J. Klimek, K. Poturaj, W. Urbanczyk, T. Nasilowski, F. Berghmans, and H. Thienpont, "Highly birefringent microstructured fibers with enhanced sensitivity to hydrostatic pressure," Opt. Express **18**(14), 15113–15121 (2010).
14. P. Zu, P. L. So, and C. C. Chan, "An Ultrahigh Sensitivity Point Temperature Sensor Based on Fiber Loop Mirror," IEEE J. Sel. Top. Quantum Electron. **23**(2), 1–4 (2017).
15. J. Ma, Y. Yu, and W. Jin, "Demodulation of diaphragm based acoustic sensor using Sagnac interferometer with stable phase bias," Opt. Express **23**(22), 29268–29278 (2015).
16. S. W. Jun, H. D. Lee, and C. S. Kim, "Optical phase-shift interrogation method with a single-ended PM-PCF sensor," IEEE Photonics Technol. Lett. **27**(11), 1185–1188 (2015).
17. H. Chen, S. Zhang, H. Fu, B. Zhou, and N. Chen, "Sensing interrogation technique for fiber-optic interferometer type of sensors based on a single-passband RF filter," Opt. Express **24**(3), 2765–2773 (2016).
18. M. K. Szczurowski, T. Martynkien, G. Statkiewicz-Barabach, W. Urbanczyk, and D. J. Webb, "Measurements of polarimetric sensitivity to hydrostatic pressure, strain and temperature in birefringent dual-core microstructured polymer fiber," Opt. Express **18**(12), 12076–12087 (2010).

## 1. Introduction

Optical fiber Sagnac interferometer (OFSI) sensor based on high-birefringence (HiBi) fiber has been widely used for temperature, strain, torsion, pressure, ultrasonic, magnetic field and biochemical measurement due to its distinctive advantages including simple design, ease of manufacture, low insertion loss and higher anti-noise ability in comparison to other types of fiber optic sensors [1–9]. Normally, an OFSI sensor consists of a HiBi fiber and a 3-dB coupler. The former introduces optical path difference of the two counter-propagating waves and causes an interferential spectrum, which is used as the sensing element. Until now, the interrogation method for this type of sensor is mainly based on observing the peak/dip wavelength shift. Unfortunately, the free spectrum range (FSR) limits the observable wavelength range such that there must be a tradeoff between the sensitivity and the measurable range for this interrogation method. Although the sensitivity of the OFSI sensors has been greatly improved in past few decades [10–14], the conventional interrogation method still restricts its practical application. Actually, some new demodulation methods have been put forward but they are too complex and only suit for some special systems [15–17].

In this work, we propose and demonstrate a novel interrogation method based on birefringence demodulation which is universal for all OFSI based sensors. Both the theoretical analysis and experimental verification are implemented and they prove the proposed method can precisely demodulate the measurand with great linearity in full measurable range. Besides, this method has an unlimited linear measurement range theoretically. The proposed new interrogation method is critical for OFSI based sensors and it might greatly enhance the availability of this type of sensors in practical application.

## 2. Theory of the birefringence demodulation based method

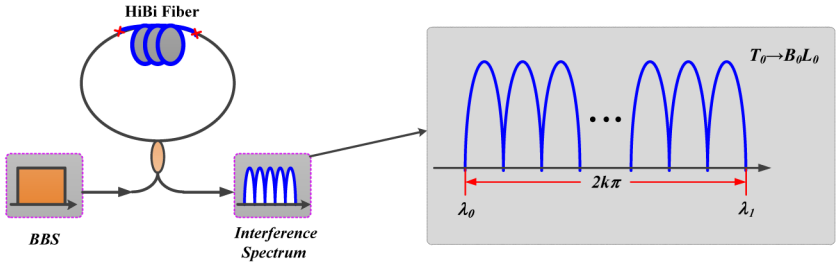


Fig. 1. The schematic of an optical fiber Sagnac interferometer based sensor.

Figure 1 shows the schematic of a conventional OFSI sensor, it includes a broadband light source (BBS), a 3 dB single-mode fiber coupler and a piece of HiBi fiber. The optical intensity transmission ($T$) of the fiber loop is approximately a periodic function of the

Optics EXPRESS

wavelength with a spacing between adjacent transmission peaks of $S = \lambda^2/BL$ (which is named FSR) and is given by [5]

$$T = \frac{(1-\cos\varphi)}{2} \tag{1}$$

where $\varphi = 2\pi BL/\lambda$ is the phase difference between the two counter-propagating beams caused by the birefringence of the fiber, $B$ is the birefringence of the HiBi fiber, $L$ is the length of the HiBi fiber, $\lambda$ is the wavelength. As shown in Eq. (1), the transmission function is decided by the product of $BL$ and wavelength. Generally, the wavelength does not change once being established. That means the transmission spectra is only decided by the product of $BL$. Meanwhile, the value of $BL$ is linearly proportional to measurand (such as temperature, strain and pressure etc.). As shown in Fig. 1, the phase difference ($\Delta\varphi = |\varphi_0-\varphi_1|$) of the transmission spectra at two different wavelength $\lambda_0$ ($\varphi_0 = 2\pi BL/\lambda_0$) and $\lambda_1$ ($\varphi_1 = 2\pi BL/\lambda_1$) can be described as

$$\Delta\varphi = \frac{2\pi BL(\lambda_1-\lambda_0)}{\lambda_0\lambda_1} \tag{2}$$

Therefore, the $BL$ can be calculated through measuring the two wavelength if fixing the phase difference $\Delta\varphi$ to $2k\pi$ ($k$ is a positive integer). Note that, $k$ can be adjusted and its maximum is restricted by the bandwidth of the optical source (see the Fig. 1). And the Eq. (2) can be rewritten as

$$BL = \frac{k\lambda_0\lambda_1}{(\lambda_1-\lambda_0)} \tag{3}$$

As proved in previous investigation, $BL$ is linearly proportional to the measurand [1–5]. Therefore, the measurable range of this demodulation method is unlimited theoretically. That has a huge advantage over the conventional demodulation method with peak/dip wavelength observation.

## 3. Experimental setup and results

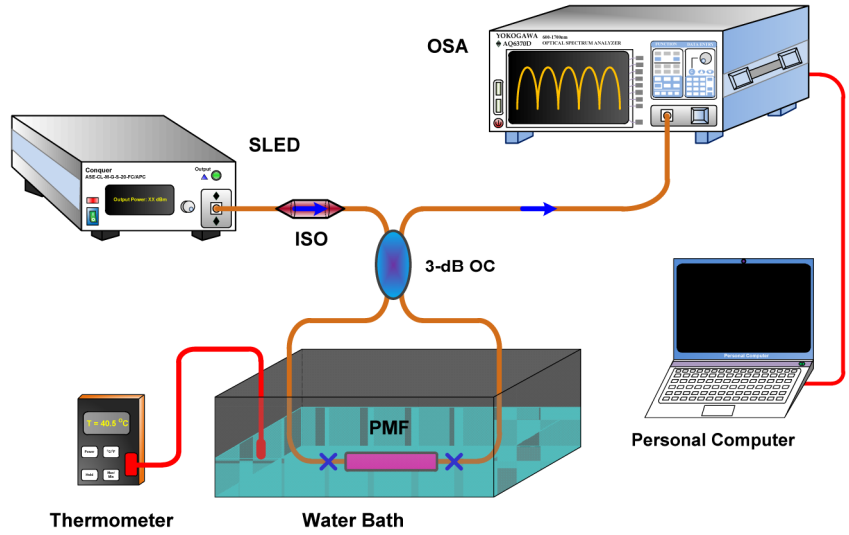


Fig. 2. Experimental setup. SLED: superluminescent light-emitting diode; ISO: isolator; OC: optical coupler; PMF: polarization maintaining fiber; OSA: optical spectrum analyzer.

Optics EXPRESS

In order to verify the feasibility of the proposed interrogation method, a normal Sagnac loop interferometer scheme based on polarization maintaining fiber (PMF) was implemented for temperature measurement and its experimental setup is shown in Fig. 2. A broadband superluminescent light-emitting diode (SLED) source with 80 nm bandwidth is used as a light source. After being split through a 3 dB single-mode fiber coupler, the two equal branches are injected into 67-cm panda-type PMF (PM1550, 125-18/250), which is provided by Yangtze Optical Fiber and Cable Company Ltd. (YOFC) and its phase modal birefringence B is about $6.9 \times 10^{-4}$. At last, the raw data is collected and processed with an optical spectrum analyzer (OSA) and a personal computer, respectively. In experiment, we adopted water bath method to heat the sensing element (PMF) and a thermometer was acted as the reference.

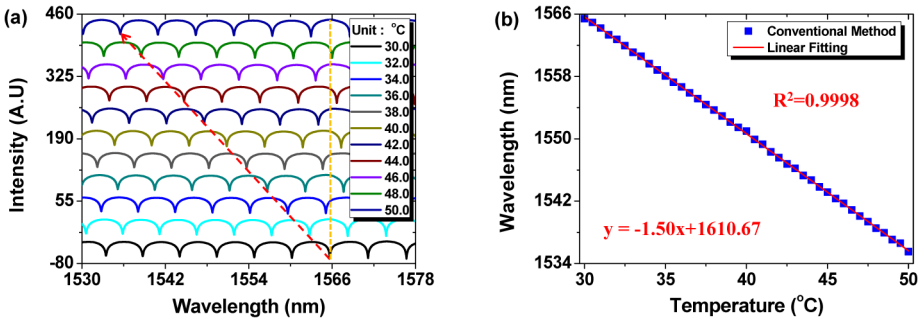


Fig. 3. The demodulation results with conventional method. (a) The dip wavelength shift to shorter wavelength with the temperature increase. (b) The test results and the fitting curve by using the conventional method.

For the demodulation of OFSI based sensor, the conventional method is based on tracking peak/dip wavelength shift. To precisely demodulate the temperature, high sampling interval of 0.0016 nm has been adopted in the experiment. Figure 3(a) shows the change of the dip wavelength with the increase of the test temperature (see the red dash line in Fig. 3(a)). To clearly depict the linear relation of the dip wavelength and temperature, the test results and their fitting curve are illustrated in Fig. 3(b). It is noted that Figs. 3(a) and 3(b) are the same results except that Fig. 3(a) just shows part results (temperature increases with step of 2 °C) but Fig. 3(b) shows all the results (temperature increases with step of 0.5 °C). Obviously, the conventional method can accurately demodulate the measurand. But the interference spectrum is approximately a periodic function of the wavelength (as explained in section 2) so that multiple temperatures correspond to a same dip wavelength (see the yellow dash line in Fig. 3(a)). Therefore, the conventional method can be used to test sensor's characteristic in laboratory (like the result shown in Fig. 3(b)) but it is not suitable for practical application.

In practice, the measurable range of the conventional method is limited by FSR (the FSR in this experiment is about 5.39 nm). As shown in Fig. 4(a), the dip wavelength shifts from 1555 to 1549 nm, with the temperature increasing gradually from 30 °C to 33.5 °C. Moreover, the interference spectrums will overlap if temperature beyond 33.5 °C due to the feature of periodic function. To more clearly display the limitation of the conventional method, Fig. 4(b) shows the dip wavelength shift in one FSR when temperature increases from 30 to 50 °C with step of 0.5 °C. As illustrated in Fig. 4(b), multiple temperatures correspond to a same dip wavelength. That makes it impossible to determine which one is the real temperature for the conventional method.

Optics EXPRESS

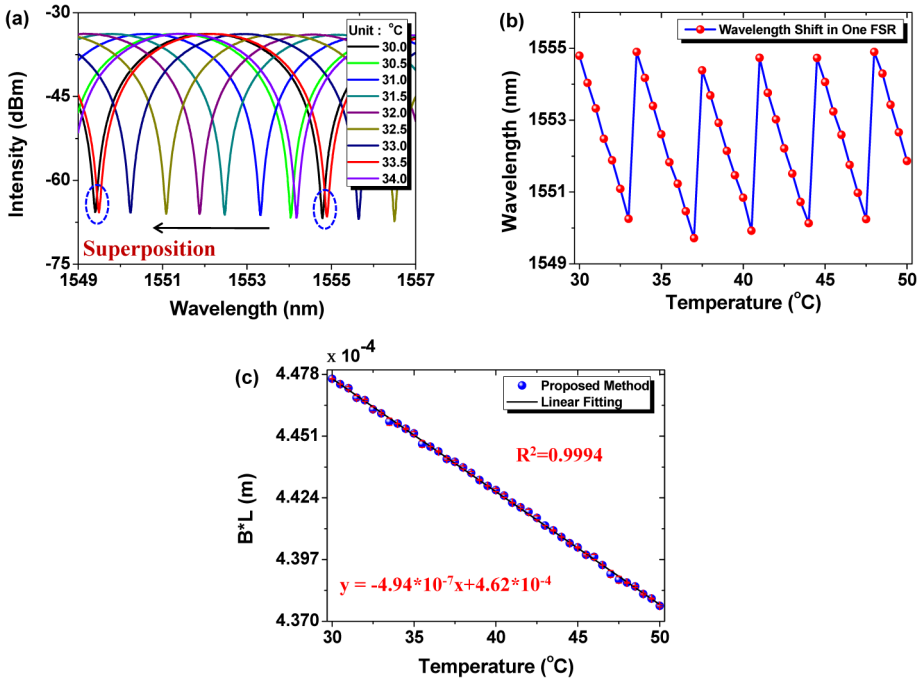


Fig. 4. The comparison of the conventional method and the proposed method with a 0.67-m PMF, the test temperature increases from 30 °C to 50 °C with step of 0.5 °C. (a) The change of interference spectrum with temperature increase in one FSR. (b) The dip wavelength shift when temperature increases in one FSR. (c) The variation of *BL* when temperature increases.

Different from the conventional demodulation method, the proposed method is based on *BL* demodulation and there is a one-to-one correspondence between the *BL* and the measurand. In addition, the *BL* is the fiber's property and it is proportional to the measurand with a great linearity in full measureable range. To verify this property, same raw data as above (shown in Figs. 3 and 4) was processed with the proposed method and the corresponding result is shown in Fig. 4(c). Consistent with theoretical analysis, the *BL* is linearly proportional to the temperature with a negative coefficient in full test range and the demodulation results have a good linearity of 0.9994. Besides, the fiber length in OFSI based temperature sensor can be regarded as a constant [1,3,10,11]. So, the expression of the birefringence and temperature can be rewritten as $B = -7.38 \times 10^{-7} \times T + 6.90 \times 10^{-4}$ (T is the temperature). The coefficient of $dB/dT$ ($-7.38 \times 10^{-7}$) and the $B_0$ ($6.90 \times 10^{-4}$) are in good agreement with the fiber's property. Moreover, the sensitivity (temperature, pressure, strain) can be further improved through adopting special optical fiber such as the birefringent microstructured fiber [13] and the microstructured polymer fiber [18]. Compared to the conventional method, as illustrated in Fig. 4(b), the proposed method extends sensing range to original six times.

Optics EXPRESS

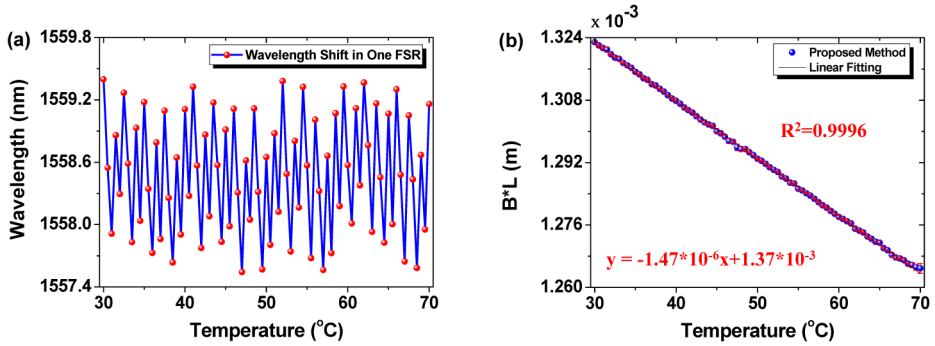


Fig. 5. The comparison of the conventional method and the proposed method with a 2-m PMF. (a) The change of the dip wavelength shift in one FSR and (b) the variation of *B*L* when the test temperature increases from 30 °C to 70 °C with step of 0.5 °C.

In theory, the measurable range of this proposed method is unlimited due to it is only decided by *BL* (which is the fiber's property). To verify the unlimited measurable range of this demodulation method, another experiment with longer fiber length (2-m PMF with same property as the shorter PMF used in former test) and wider temperature range from 30 °C to 70 °C with increasing step of 0.5 °C has been accomplished. As illustrated in Fig. 5(a), there is a narrower measurable range for the conventional demodulation method since the longer sensing fiber will reduce FSR. In contrast, the measurable range of the proposed method is not affected by FSR. As illustrated in Fig. 5(b), the demodulation result is directly proportional to the temperature with a negative coefficient in full range and an excellent linearity of 0.9996 has been achieved. Compared to the conventional method, it improves the measureable range to original over 30 times. According to the theoretical analysis and the experiment tests, the measurable range of this method is indeed unlimited.

## 4. Discussions

In addition, demodulation error and its affecting factors are very important for the proposed demodulation method. According to the Eq. (3), the demodulation precision is mainly decided by the measurement accuracy of dip wavelength. Therefore, we introduce the measurement error of dip wavelength ($\delta\lambda$) into Eq. (3) and rewrite it as

$$\begin{aligned} BL &= \frac{k\cdot(\lambda_0 \pm \delta\lambda)\cdot(\lambda_1 \pm \delta\lambda)}{(\lambda_1 - \lambda_0 \pm 2\delta\lambda)} \\ &= \frac{k\cdot[\lambda_0\lambda_1 + \delta\lambda(\lambda_0 \pm \lambda_1) \pm \delta\lambda^2]}{(\lambda_1 - \lambda_0 \pm 2\delta\lambda)} \end{aligned} \tag{4}$$

where $\delta\lambda$ is mainly caused by wavelength sampling interval and its maximum is less than the sampling interval. Considering that $\delta\lambda$ is generally far less than $\lambda_1$-$\lambda_0$ (over two orders of magnitude), the Eq. (4) can be rewritten as

$$\begin{aligned} BL &\approx \frac{k\cdot[\lambda_0\lambda_1 + \delta\lambda(\lambda_0 \pm \lambda_1)]}{(\lambda_1 - \lambda_0)} \\ &= \frac{k\lambda_0\lambda_1}{(\lambda_1 - \lambda_0)} + \left[\frac{k\cdot\delta\lambda(\lambda_0 \pm \lambda_1)}{(\lambda_1 - \lambda_0)}\right] \end{aligned} \tag{5}$$

In Eq. (5), the first component is desired (same as the Eq. (3)) but the second component (in bracket) is the demodulation error introduced by wavelength error. To precisely demodulate the measurand, we will discuss the influence factors for the demodulation error from two aspects of wavelength sampling interval and wavelength span.

Optics EXPRESS

### 4.1 The influence of the wavelength sampling interval

According to Eq. (5), the demodulation error is directly proportional to the wavelength error ($\delta\lambda$). We assume that $\delta\lambda$ equals to the wavelength sampling interval due to the maximum $\delta\lambda$ is limited by the wavelength sampling interval (and it is less than the sampling interval). Thus, the overall trend of the demodulation error is proportional to the sampling interval. Meanwhile, a simulation with same parameters as the experiment parameters has been implemented to compare with the test results.

The theoretical simulation is implemented with the Matlab software. The optical intensity transmission function is shown in Eq. (1), where the temperature mainly changes the B. The phase modal birefringence and temperature sensitivity are $B_0 = 6.9 \times 10^{-4}$ and $dB/dT = -7.4 \times 10^{-7}$, respectively. The simulation process is as follows:

(1) Obtaining the transmission spectra according to Eq. (1);

(2) Calculating the corresponding BL utilizing Eq. (3) and the transmission spectra;

(3) Tuning the B according to the expression of $B = B_0\text{-}T \times (dB/dT)$;

(4) Repeating the step 1 to step 3 till the cut-off temperature;

(5) Calculating the $R^2$ with all test temperatures (T) and their corresponding BL.

It should be noted that the $R^2$ is calculated with the function of *polyfit(x,y,n)*, which is a standard curve fitting function based on the least square method.

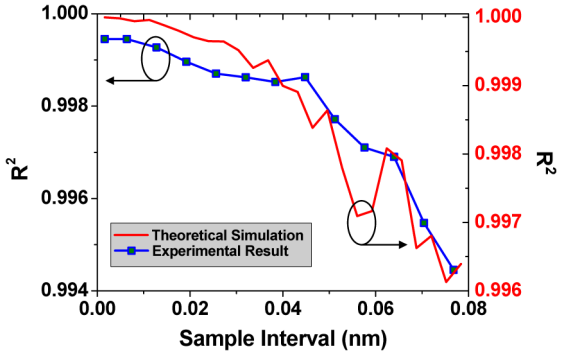


Fig. 6. The influence of the wavelength sampling interval on demodulation error, where the red solid line and the blue dot line are the theoretical simulation and experimental result, respectively.

In this work, $R^2$ acts as the standard of demodulation error and the demodulation error increases with $R^2$ reduction. Under the condition of keeping other parameters unchanged (the fiber length and the wavelength span are fixed at 0.67 m and 80 nm, respectively), simulation and experiment have been implemented through increasing the sampling interval from 0.0016 nm to 0.0784 nm with step of 0.0064 nm. Figure 6 shows that the $R^2$ reduces with the sampling interval increase both in theoretical simulation (the red solid line) and experimental results (the blue dot line), respectively. That means the demodulation error increases as the sampling interval increasing. Note that, the judder of the simulation (red solid line) and experiment (blue dot line) is normal since the real wavelength error is random and less than the wavelength sampling interval.

### 4.2 The influence of the wavelength span

From the Eq. (5), the variation of the wavelength span ($\lambda_1$-$\lambda_0$) will change the demodulation error. Meanwhile, the increase of the wavelength span will enlarge $k$, so that the demodulation error is determined by the ratio of $k/(\lambda_1\text{-}\lambda_0)$. In the ratio, $k = (\lambda_1\text{-}\lambda_0)/S$ and the

Optics EXPRESS

ratio equals to *1/S*. Moreover, *S* (the spacing between adjacent transmission peaks which is the FSR) increases with the wavelength addition [1–5]. That means the ratio of $k/(\lambda_1-\lambda_0)$ reduces as the span increasing that results in the demodulation error decreasing. In conclusion, the demodulation error reduces with the wavelength span increasing.

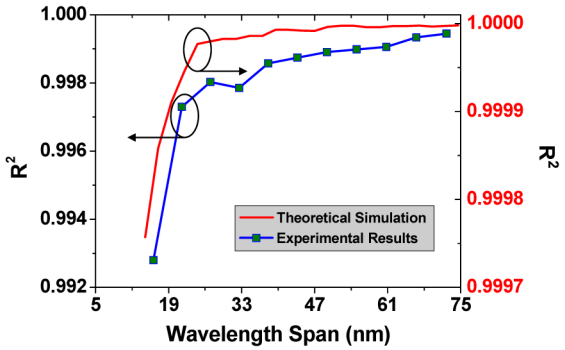


Fig. 7. The influence of the wavelength span on the demodulation error, where the red solid line and the blue dot line are the theoretical simulation and experimental results, respectively.

Similar to above section, only the wavelength span was tuned from 16.1 nm to 72.3 nm with step of ~5.6 nm. Other parameters keep constant such as the fiber length and the sampling interval are fixed at 0.67 m and 0.0016 nm, respectively. It should be noted that the tuning step of the wavelength span should be larger than the FSR (~5.4 nm). As shown in Fig. 7, it is obvious that $R^2$ increases as the span increasing and the experiment agrees well with the simulation. That is to say, the demodulation error reduces with the wavelength span increase (which is coincident with the theoretical analysis illustrated in Eq. (5)).

## 5. Conclusion

We propose and experimentally demonstrate a novel demodulation method based on birefringence demodulation for Sagnac interferometer based sensor. An OFSI based temperature sensor has been implemented to verify the feasibility of the proposed method. Test temperature increasing from 30 °C to 70 °C with step of 0.5 °C has been accurately demodulated with a great linearity of 0.9996. Especially, the proposed method overwhelms the conventional method due to it suits for all OFSI sensors and has an unlimited linear range theoretically. In addition, the new method has a great significance for the OFSI based sensor and it might greatly improve the practicability of this type of sensors.

## Funding

International Science and Technology Cooperation Program of China (2014DFA11170); National Natural Science Foundation of China (No. 61475128); Key Grant Project of Chinese Ministry of Education (No. 313049); Fundamental Research Fund for the Central Universities (2682014RC22).